Biochimica et Biophysica Acta 1838 (2014) 3130–3136

Contents lists available at ScienceDirect

Biochimica et Biophysica Acta

journal homepage: www.elsevier.com/locate/bbamem

Molecular resolution visualization of a pore formed by trichogin, an antimicrobial peptide, in a phospholipid matrix

Maxim Smetanin [a], Slawomir Sek [a,b], Flavio Maran [c], Jacek Lipkowski [a,*]

[a] Department of Chemistry, University of Guelph, Guelph, ON N1G 2W1, Canada
[b] Faculty of Chemistry, Biological and Chemical Research Centre, University of Warsaw, Zwirki i Wigury 101, 02-089 Warsaw, Poland
[c] Department of Chemistry, University of Padova, Via Marzolo 1, 35131 Padova, Italy

ARTICLE INFO

Article history:
Received 10 March 2014
Received in revised form 5 August 2014
Accepted 7 August 2014
Available online 23 August 2014

Keywords:
Trichogin
Antimicrobial peptide
Barrel-stave model
Peptide aggregation
Scanning tunneling microscopy

ABSTRACT

Electrochemical scanning tunneling microscopy (EC-STM) was employed to study the aggregation of trichogin OMe (TCG), an antimicrobial peptide, incorporated into a lipid monolayer. High-resolution EC-STM images show that trichogin molecules aggregate to form channels in the lipid monolayer. Two types of aggregates were observed in the images. The first consisted of a bundle of six TCG molecules surrounding a central pore. The structure and dimensions of this channel are similar to aggregates that in bilayers are described by the barrel-stave model. The EC-STM images also reveal that channels aggregate further to form a hexagonal lattice of a two dimensional (2D) nanocrystal. The model of 2D lattice was built from trimers of TCG molecules that alternatingly are oriented with either hydrophilic or hydrophobic faces to each other. In this way each TCG molecule is oriented partially with its hydrophilic face towards the hexameric pore allowing the formation of the column of water inside this pore.

1. Introduction

Antimicrobial peptides (AMPs) are important components of the innate immunity which is the first line of defense of all organisms, including plants and humans [1]. AMPs have typically 12–50 amino acids and about 50% of them are hydrophobic [1–3]. They are involved in antiseptic, immunomodulatory and chemotactic processes [4]. AMPs are mobilized immediately after microbial infection and are able to rapidly neutralize a broad range of microbes [5]. They aggregate in the cellular membrane of pathogens and form pores leading to cell death as a result of the osmotic shock and leakage of intracellular content [4,5]. Possible mechanisms of pore formation by AMPs have been proposed on the basis of barrel-stave, toroidal, and carpet models [3].

Due to its unique features, trichogin provides a very interesting case of AMP. Trichogin-OMe, [6] (TCG) is an 11 residue peptide with the following sequence:

N-term 1 2 3 4 5 6 7 8 9 10 11 C-term

n-Oct-Aib-Gly-Leu-Aib-Gly-Gly-Leu-Aib-Gly-Ile-Leu-OMe

It is an analog of trichogin GA IV isolated from fungus *Trichoderma longibrachiatum* [7] in which leucinol is replaced by leucine methyl ester (Leu-OMe) [6,8]. The structure of TCG combines distorted 3_{10}-helix (residues 1 to 3) with irregular α-helix formed from 5 to 11 residues [7,9–11] with all side chains of hydrophobic groups located on one side of the helix (*n*-octanoyl, Ile_{10}, $Leu_{3,7}$ and Leu-OMe) and four hydrophilic $Gly_{2,5,6,9}$ residues located on the opposite side of the helix [10]. The methyl groups of α-aminoisobutyric acid (Aib) residues $Aib_{1,4,8}$ are aligned along the borderline between the two helical fragments. Although trichogin is a linear peptide, its size at the N- and C-termini is different due to the presence of the *n*-octanoyl group at the N-terminus. According to the crystallographic data [10], the length of TCG is 2.0 ± 0.1 nm and its diameters at the N- and C-termini are 1.0 ± 0.1 and 0.9 ± 0.1 nm, respectively. Trichogins belong to the sub-class of peptabiotics termed lipopeptaibols [12]. The amphiphilic character of trichogins determines their antibiotic activity. The peptide shows a good activity against Gram-positive bacteria like *Staphylococcus aureus* strains and stability towards proteolytic degradation [13,14]. These properties make trichogins promising candidates in therapeutic treatments.

The position and orientation of trichogin and its analogs in model membranes have been studied using pulsed electron–electron double resonance (PELDOR) [15,16], fluorescence spectroscopy [17,18], and electron spin echo [19]. The effect of trichogin incorporation on the molecular properties of the membrane was investigated by multinuclear solid-statenuclear magnetic resonance (NMR), Fourier transform infrared absorption spectroscopy (FT-IR) [20], and neutron reflectivity [21]. These results showed a significant decrease in the membrane thickness

Abbreviations: AMPs, antimicrobial peptides; TCG, trichogin; DMPC, 1,2-dimyristoyl-sn-glycero-3-phosphocholine; EC-STM, electrochemical scanning tunneling microscopy; NMR, nuclear magnetic resonance; FT-IR, Fourier transform infrared absorption spectroscopy

* Corresponding author.
E-mail address: jlipkows@uoguelph.ca (J. Lipkowski).

http://dx.doi.org/10.1016/j.bbamem.2014.08.006
0005-2736/

with increasing trichogin concentration [21]. At low concentrations the peptides lie just below the polar head region, parallel to the membrane surface [16,19]. At higher concentrations the peptide molecules aggregate and insert deeply inside the membrane, causing membrane leakage [4,18]. In particular, electron paramagnetic resonance studies [16,19] indicated that an increase of TCG concentration causes an orientation change resulting in the N-terminus of the peptide buried deeper inside the membrane forming head-to-head transmembrane dimers [19]. The leakage of unilamellar vesicles has been observed at peptide to lipid (P:L) ratios between ~5×10^{-3} and 2×10^{-3} for vesicles made of eggPC [6] and 1:1 eggPC and cholesterol mixture [22]. Measurements of the rate constant for ion diffusion across the membrane (k) in the presence of trichogin showed that k depends on TCG concentration to power N ($k \propto \mathrm{TCG}]^N$), where N, estimated to be between 3 and 4, is the number of peptide molecules forming the transmembrane channel [23]. Recently, TCG was incorporated into a bilayer tethered to a Hg electrode surface and observed that peptide molecules aggregate to form voltage-gated channels similar to those exhibited by the peptaibol alamethicin [24]. Although, there is a significant body of evidence that at sufficient P:L ratios TCG is inserted into the membrane and that in the inserted state peptide molecules aggregate to form an ion conductive pore, the exact structure of this pore is still unknown.

The objective of this work is to apply electrochemical scanning tunneling spectroscopy (EC-STM) to image TCG aggregates in a phospholipid matrix to determine the nature of the aggregation and the structure of the aggregates. We build on our recent success to image aggregates of gramicidin [25] and alamethicin [26] in monolayers of phospholipids deposited on a gold electrode surface. High-resolution EC-STM images acquired in this study provided unique direct evidence that TCG forms pores in the 1,2-dimyristoyl-sn-glycero-3-phosphocholine (DMPC) monolayer. Similar to alamethicin [26], TCG has also a tendency to form 2D-nanocrystals of a variable size. However, due to the shorter length of the helix (ca. 2 nm), the nanocrystals of TCG have a smaller size than those formed by alamethicin (helix length of 3.2 nm) [26]. The EC-STM images revealed the presence of individual channels formed by six TCG peptide molecules in the DMPC matrix. The structure and dimensions of this channel are similar to aggregates that in bilayers are commonly referred to as the barrel-stave model. The results presented in this work are important for the understanding of the biocidal activity of TCG. The relevance of these results is also significant because trichogin is a versatile template for the synthesis of novel peptaibiotics [11,27].

Monolayers of phospholipids have been frequently used as a model to study interactions of antibacterial peptides with lipids [28]. At present, high-resolution STM images of a film of phospholipid in solution can be acquired for a monolayer only and, therefore, here we provide information concerning the peptide–lipid interaction in a monolayer. However, molecular resolution STM images of a phospholipid bilayer supported at a conductive surface in air have already been reported [29]. With further methodological improvements, imaging of the supported bilayer in a solution should also be possible.

2. Materials and methods

2.1. Surface preparation

The working electrode was a small Au bead formed by melting a gold wire (Alfa Aesar, 99.999% purity). The bead was welded to a gold plate. The atomically flat (111) facets at the bead surface were used for image acquisition. Before each experiment the gold electrode and the Kel-F parts of the STM electrochemical cell were cleaned in a piranha solution (concentrated H_2SO_4/30% H_2O_2 3:1 v/v) for at least 6 h and rinsed thoroughly with Milli-Q ultra-pure water. (*CAUTION: piranha solution reacts violently with organic materials and should be handled with extreme care*). The gold electrode was then flame annealed and quenched in Milli-Q water prior to the experiment. The EC-STM images were acquired using a Nanoscope II EC-STM connected to a Nanoscope IIIa controller (Digital Instruments, Santa Barbara, CA) with an A scanner. The constant current mode was used for imaging. The tungsten EC-STM tips were electrochemically etched in 2 M NaOH and then coated with polyethylene in order to minimize faradaic currents. The EC-STM experiments were carried out at 21 ± 1 °C. A 0.1 M NaF (MV Laboratories Inc.) solution was used as a supporting electrolyte. Milli-Q ultra-pure water (final resistivity ≥ 18.2 MΩ cm) was used to prepare all solutions. During the image acquisition, the electrode was kept at an open circuit potential (OCP) of + 0.2 V vs Ag/AgCl with a bias voltage of − 400 mV.

2.2. Langmuir–Blodgett transfer

1,2-Dimyristoyl-sn-glycero-3-phosphocholine (DMPC) (Avanti) was used without further purification. The TCG-OMe was synthesized, purified, and characterized [24] following the procedure described by Toniolo et al. [6]. These compounds were used to make 1 and 0.3 mg mL^{-1} stock solutions, respectively, in chloroform (Sigma-Aldrich) solvent. Langmuir–Blodgett monolayers were prepared from both pure lipid and peptide and a 1:9 peptide/lipid solution. A few drops of each of these solutions were spread at the surface of a water-filled Langmuir–Blodgett trough (KSV LB5000, Finland) to form a corresponding monolayer. The trough was controlled by a computer using KSV LB5000 v.1.70 software. The pure or the mixed monolayer was transferred from the Langmuir trough onto the Au(111) substrate using the Langmuir–Blodgett technique at a surface pressure of 35 mN m^{-1}. During the compression and transfer of the film the temperature of the aqueous subphase was kept at 30 °C. After the deposition, the sample was dried 4 h at room temperature (~21 °C) and then transferred into the STM electrochemical cell. The EC-STM experiments were carried out at 21 ± 1 °C. This temperature coincides with the gel to liquid phase transition temperature of a monolayer of DMPC [30]. Consequently, the lipids were less ordered than in the previous study by Pieta et al. [26]. However, at this temperature we were able to observe a better order of trichogin aggregates and hence this condition was chosen in the present study. When the Langmuir–Blodgett method is used, the film transferred onto the gold surface retains its orientation from the air–solution interface. The polar head groups of DMPC interact quite strongly with the gold surface, reducing mobility of the monolayer. At the air solution interface the peptide molecules assume a tilted orientation with the hydrophilic side oriented towards the water and the hydrophobic side towards the air. When the electrode is dried in air, DMPC molecules favor the orientation with the polar heads turned towards the metal. In contrast, when peptide molecules are losing water, the tilted orientation is energetically unfavorable. In the dry state, peptide molecules aggregate into a two-dimensional structure that ensures optimum polar with polar and nonpolar with nonpolar interactions. When the electrode is immersed into the solution, the acyl chains of that film are exposed to the water. Energetically this is an unfavorable configuration. However, we did not observe the flip-flop of the molecules. Apparently, the structure of the film is stabilized by interactions between polar heads of lipids and the metal or due to the solid like nature of the film such reorganization is kinetically hindered. This behavior has already been observed by Sek et al. [25] and Pieta et al. [26].

3. Results and discussion

Prior to EC-STM experiments, the mixed 1:9 TCG–DMPC monolayer was formed at the air–solution interface of a Langmuir trough and characterized by recording compression isotherms shown in Fig. 1a. For comparison, compression isotherms for monolayers of pure DMPC and pure TCG are also plotted in this figure. The compression isotherm for pure DMPC is in agreement with published results [30,31]. The isotherm for the monolayer of TCG displays a collapse at the film pressure of ~40 mN m^{-1} and the minimum area per molecule ~1.2 nm^2. The crystallographic data indicate that the maximum packing of TCG molecules corresponds to an area per molecule of ~0.9 nm^2 for the vertical and ~2 nm^2 for the horizontal helix orientation at the interface. Therefore,

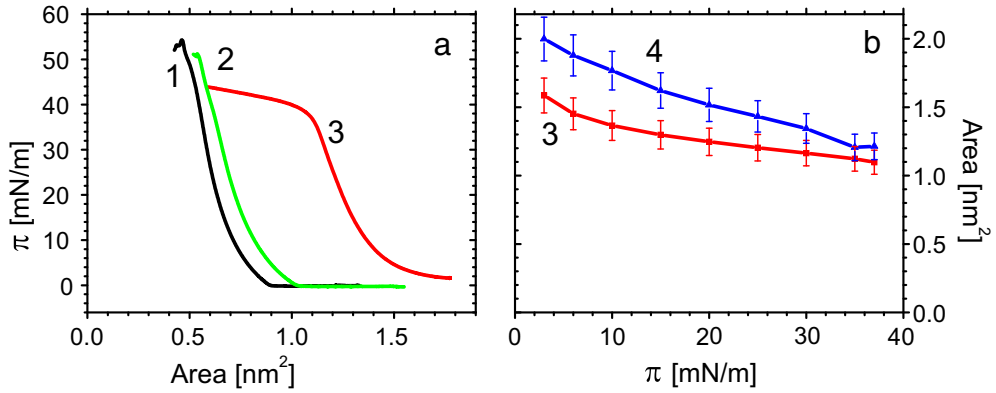

Fig. 1. Langmuir–Blodgett compression isotherms of DMPC and TCG molecules. a) Compression isotherms for: 1—pure DMPC monolayer; 2—mixed 1:9 TCG and DMPC monolayer and curve; and 3—pure TCG monolayer recorded at 30 °C of the water subphase. b) Area per TCG molecule in the mixed monolayer determined using Eq. (1). For comparison the data from compression isotherm of a monolayer of pure TCG are also plotted as curve 3. The error bars represent reproducibility of three independent measurements.

the compression isotherm suggests that TCG molecules change orientation from horizontal to tilted, upon compression. Curve 4 in Fig. 1b plots the area per one TCG molecule in the mixed monolayer (A_{TCG}) calculated with the help of the formula:

$$A_{TCG} = \frac{A_2 - 0.9A_1}{0.1} \quad (1)$$

where for a given film pressure A_2 is the mean area per molecule taken from the compression isotherm of the mixture and A_1 is the area per molecule in the monolayer of pure DMPC (curve 1 in Fig. 1a). For comparison the area per molecule in the pure monolayer of TCG is also plotted in Fig. 1b. For an ideal mixture the two curves should coincide. The data show that the area per one peptide molecule is larger in the mixture than in the monolayer of pure TCG. This behavior suggests that the peptide and the lipid do not mix well at low film pressures and that their interactions are repulsive or that this monolayer has excluded volume due for example to a pore formation. At the film pressure of 35 mN m^{-1}, the areas per TCG in the mixture and in the pure monolayer are comparable. Its value ~1.2 nm^2 suggests that the helix assumes a tilted orientation at the interface, consistent with the inserted state of the peptide.

The monolayer was transferred from the air–solution interface onto the gold surface for EC-STM studies at this value of the film pressure (35 mN m^{-1}), with the help of the Langmuir–Blodgett technique. Using this transfer method, the polar heads of lipids are oriented to the metal and their tails to the air. The film was dried in air during ~4 h, the electrode was then transferred to the electrochemical cell of the EC-STM instrument and the cell was filled with 0.1 M NaF solution. The electrode was allowed to equilibrate with the solution for a period of about 2 h. When the Langmuir–Blodgett method is used, the film transferred onto the gold surface retains its orientation from the air–solution interface. The polar head group of DMPC interacts quite strongly with the gold surface, reducing mobility of the monolayer. At the air solution interface the peptide molecules assume a tilted orientation with the hydrophilic side oriented towards the water and the hydrophobic side towards the air. Consistent with the earlier observation [25], the monolayer becomes smoother and more ordered and the contrast in the image becomes sharper as the time proceeds. The improved stability of the piezo scanner and the improved thermal equilibrium at later times contribute to the improved quality of the EC-STM images. The ability to image an insulating molecule by EC-STM may be explained in terms of a weak coupling between electronic states in the adsorbate and in the substrate near the Fermi level that gives the adsorbate a property of an antenna capable of receiving tunneling electrons [32–34]. The electrolyte assists in ordering of the monolayer. Water molecules may play a role in tunneling through biomolecules [35]. However, the role of solvent in STM imaging in solution is still poorly understood [32,34].

Figs. 2a and b show unprocessed EC-STM images of the gold electrode surface covered by the mixed TCG:DMPC monolayer. The images consist of several ordered and disordered domains formed by molecules at the metal surface. The distinction between the contrast due to the lipid and the peptide is difficult in the disordered region, hence no attempt was made to calculate the peptide to lipid ratio from the contrast in these images. Two types of ordered domains may be identified in these images. The first consists of characteristic molecular stripes. Fig. 3a is a zoomed in image of such a domain. To get further insight into the nature of this contrast, the height distance profiles were measured in the four directions marked in Fig. 3a. The profiles taken along the direction of the bright stripes (lines 1 and 3) and the dark valleys (lines 2 and 3) are shown in Fig. 3b. These profiles show periodic changes of the contrast with periodicity of 0.5 ± 0.1 nm which corresponds well to the distance between adjacent acyl chains of DMPC molecules [25]. Looking further on these profiles one notes that line 1 is in phase with line 3 and line 2 is in phase with line 4. However, lines 1 and 3 are phase shifted by ~0.5 nm with respect to lines 2 and 4. To explain this behavior Fig. 3c shows an EC-STM image of a well-ordered DMPC monolayer transferred onto the gold surface at the film pressure of ~40 mN m^{-1} and measured at 17 °C where the monolayer is in the gel state. The bright spots in this contrast are formed by well-ordered nearly vertically oriented acyl chains. Fig. 3d shows profiles along two lines marked in Fig. 3c. They show regular periodicity of ~0.5 nm, consistent with the diameter of an acyl chain, and they also show that the periodicity of the two profiles is phase shifted by 0.5 nm. To further confirm this interpretation, Fig. 3e shows an image of less ordered monolayer of pure DMPC (without peptide and measured at 18 °C) that shows similar stripes as those in Fig. 3a for the DMPC–TCG monolayer. The profiles in Fig. 3f show that periodicity observed on the bright rims and dark valleys of these stripes is similar to that observed in Fig. 3b. These numbers indicate that the stripes are formed by DMPC molecules as schematically shown by a cartoon in the inset of Fig. 3a where the head groups are oriented towards the electrode surface while the ends of acyl chains are exposed to the electrolyte. In a DMPC molecule the β-chain is shorter than the γ-acyl chain by 0.25 nm, which corresponds to a one zig-zag unit of the acyl chain [36]. Our previous IR studies, however, showed that DMPC molecules in a monolayer oriented towards the Au(111) surface are tilted by ~25° with respect to the substrate normal [37]. The contrast in Fig. 3a may be explained by a tilted packing of phospholipid molecules with the end of one acyl chain being better visible in the EC-STM images.

The second domain consists of quasi-hexagonal spots seen on the left hand side of Fig. 2a and on the upper right corner of Fig. 2b. Fig. 4a is a zoomed in image of this type of domains. The hexagons are arranged into a two dimensional (2D) crystallographic lattice. Fig. 4b shows that

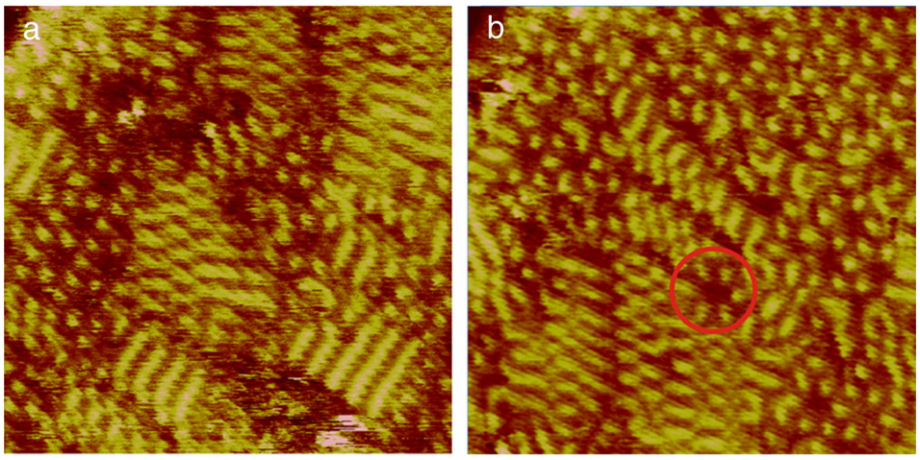

Fig. 2. 20 × 20 nm^2 molecular resolution EC-STM images of the mixed 1:9 TCG:DMPC monolayer in 0.1 M NaF electrolyte recorded at 200 mV vs Ag/AgCl, 350 pA tunneling current, 400 mV bias voltage, and 21 °C temperature.

the unit vector of this lattice has a dimension of 1.9 ± 0.1 nm and the angles between the vectors are 60 ± 5° and 120 ± 5°. The average area of the cell is equal to 3.1 ± 0.3 nm^2. Each cell of this lattice contains three spots. These are dimensions of a hexagonal lattice and this structure is similar to the structure of 2D nanocrystals formed by another lipopeptaibol — alamethicin [26] in a lipid matrix. The sizes of spots that form this pattern are variable but could be fit into a circle with a radius of ~0.45 nm. This number corresponds well to the radius of trichogin at its N-terminus. The distance between the adjacent spots of the hexagons, about 1 nm, is in agreement with the distance between trichogin molecules measured in a racemic crystal by X-Ray crystallography [10]. Therefore, we can safely conclude that this pattern is caused by aggregated peptide molecules. The contrast shows that six spots in this pattern surround a central hole. In Fig. 4c the cross sectional profiles along directions 1 and 2 (see Fig. 4a) show that the width of the central pore is ~1.9 nm. The cross section along line 3 shows that the distance between peptide molecules is ~0.9 nm. To emphasize this point in Fig. 4b each group of six spots is enclosed in a circle with a radius of 0.95 nm. This number is equal to the sum of the radius of the hole and half of the radius of the peptide. These numbers are consistent with the dimensions of the pore formed by alamethicin molecules [26] and with the size of the pore needed for the passage of hydrated potassium ion [38]. In the EC-STM images of the mixed monolayer a similar contrast is observed for DMPC and TCG molecules. As mentioned earlier, the contrast may be explained in terms of a weak coupling between electronic states in the adsorbate and in the substrate near the Fermi level that gives the adsorbate a property of an antenna capable of receiving tunneling electrons [32–34]. In the present case the length of TCG molecule is 2.0 ± 0.1 nm [10] and the length of the DMPC molecule is ~2.7 nm [1]. In a tilted orientation of DMPC molecules the two "antennas" have a comparable length. Finally, we note that we made an attempt to image a pure TCG monolayer. However, the interactions between the peptide molecules and the gold electrode were too weak and the peptide molecules were moved by the STM tip.

The contrast in Figs. 4a and b suggests that each TCG molecule is shared by two channels. This is again similar to the case of alamethicin

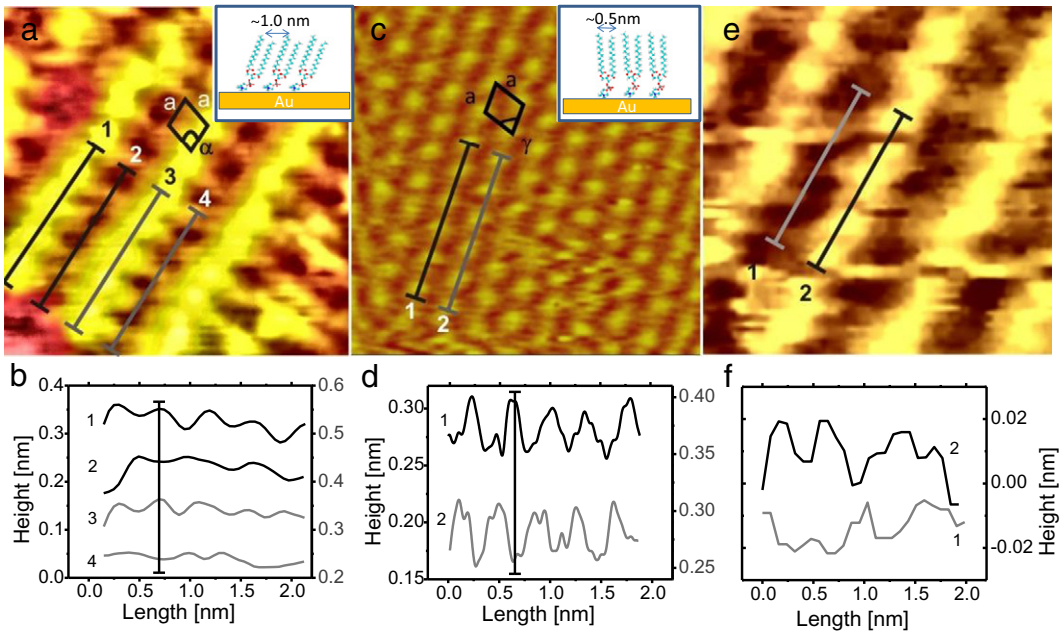

Fig. 3. Structure of the lipid domains. a) A 8 × 8 nm^2 EC-STM image of a stripe like domain in the mixed 1:9 TCG :DMPC monolayer at the Au(111) surface; b) cross sectional profiles along of the bright stripes (lines 1 and 3) and along the valleys between the stripes (lines 2 and 4); c) EC-STM image of a well ordered monolayer of pure DMPC in the gel state; d) cross sectional profiles taken along lines 1 and 2 marked in panel c; e) EC-STM image of a monolayer of pure DMPC in a partially disordered state; and f) cross sectional profiles taken along directions 1 and 2 marked in panel e.

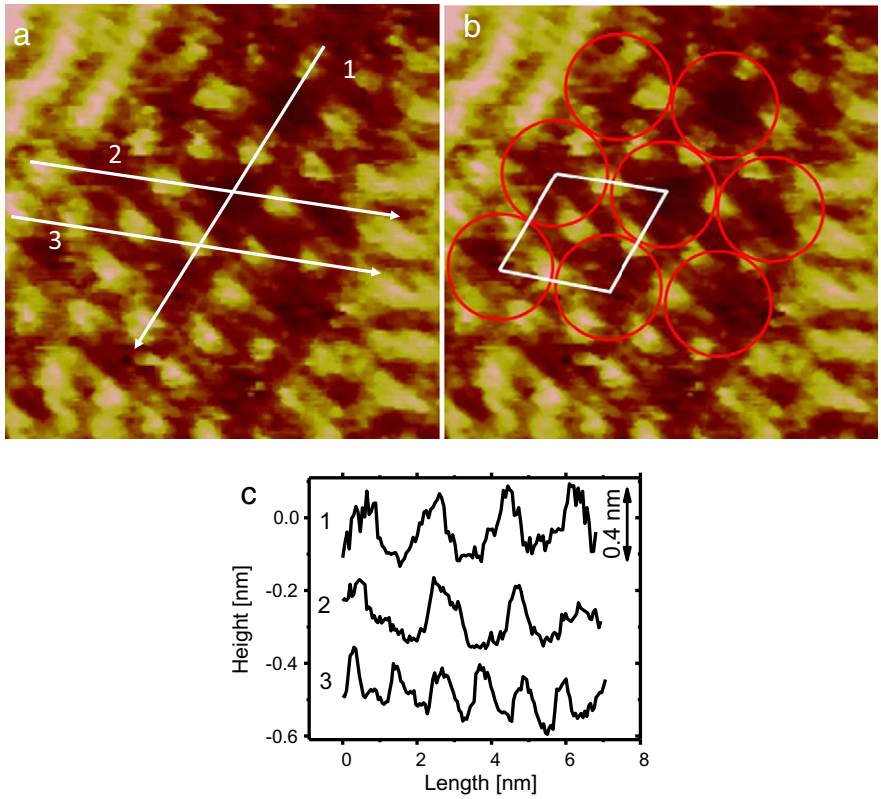

Fig. 4. STM image of a peptide domain. a) A 8 × 8 nm^2 EC-STM image of an ordered domain formed by aggregates of trichogin molecules. b) The same image with unit cell of the two dimensional lattice whose two vectors are 1.9 ± 0.1 nm long and angles between the vectors are 60 ± 5° and 120 ± 5°. The circles with 1 nm radius illustrate that the contrast in this image may be interpreted as a cluster of barrel-stave pores formed by trichogin in the DMPC monolayer. c) Cross sectional profiles taken along lines indicated in panel a. Images acquired in 0.1 M NaF electrolyte at 200 mV vs Ag/AgCl, 350 pA tunneling current, 400 mV bias voltage, and 21 °C temperature.

[26]. Using crystallographic data [10], the electrostatic surface potential representation of TCG molecule is plotted in Fig. 5a. The structure was rendered with PyMOL software [39]. The red and blue colors mark hydrophilic and green marks hydrophobic fragments of the molecule surface. The models show hydrophobic and hydrophilic sides of the peptide and the electrostatic surface potential on its N- and C-termini. These models show that hydrophilic residues are located on one side of TCG molecule and that its C-terminus is hydrophilic while the rest of the peptide surface and its N terminus are hydrophobic. This information was used to build a molecular model in Fig. 5b that explains the contrast in the EC-STM image. In this model, dimensions of the peptide molecules that fit the contrast are consistent with the crystallographic data. The central pore is surrounded by 6 peptide molecules. Fig. 5c illustrates schematically how this packing optimizes hydrophobic–hydrophobic and hydrophilic–hydrophilic interactions between the peptide molecules. In fact, the 2D lattice is built from trimers of TCG molecules that alternatingly are oriented with either hydrophilic or hydrophobic faces to each other. In this way each TCG molecule is oriented partially with its hydrophilic face towards the hexameric pore allowing the formation of the column of water inside this pore. This is consistent with the crystallography. A unit cell of the 2D lattice shown in Fig. 5b contains one pore and three peptide molecules. In the models of Figs. 5b and c the lattice has both hexameric and trimeric hydrophilic pores. Incidentally, this is consistent with previous estimates of 3 to 4 trichogins participating in the formation of the ion conducting channel [23,40]. In the model Fig. 5b the TCG molecules were oriented with the hydrophilic C

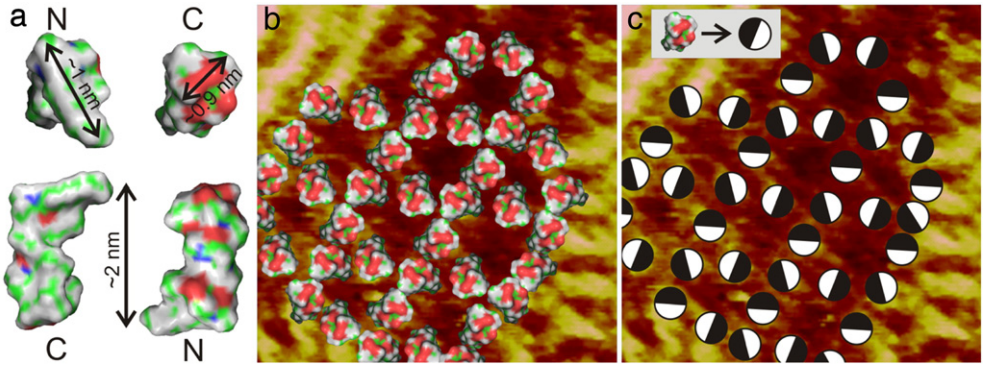

Fig. 5. Structure of pores formed by TCG molecules. a) The electrostatic surface potential profiles of TCG molecule calculated and rendered using the APBS PyMol plugin [39]. The four models show the profiles on the hydrophobic and hydrophilic sides of the molecule and the corresponding top views of the N- and C-termini, respectively. The red color marks hydrophilic and green hydrophobic fragments of the molecule surface. b) Proposed structural model for the TCG molecule assembly superimposed on the 8 × 8 nm^2 EC-STM image recorded at 200 mV vs Ag/AgCl, 350 pA tunneling current, 400 mV bias voltage, and 21 °C temperature. c) A schematic diagram showing how the hydrophobic–hydrophobic and hydrophilic–hydrophilic interactions are optimized in the molecular model of panel b; open half circles represent the hydrophilic face of the peptide and black half circles represent the hydrophobic face.

terminus towards the aqueous phase and the hydrophobic N terminus towards gold. Alternatively, TCG molecules may assume the opposite orientation. Although, we do not have strong arguments in favor of one of the two orientations, the model in Fig. 5b shows nicely that a water rich pore may be formed by the aggregates.

The TCG aggregation is very similar to the aggregation of alamethicin molecules. However, in the case of TCG the aggregates are much smaller and less ordered. Apparently, the peptide–peptide interactions are weaker in the case of TCG molecules whose helix (2 nm) is shorter than the helix of alamethicin molecule (~3.2 nm long). Due to the weaker peptide–peptide interactions, not only aggregates but also individual pores can be observed in the EC-STM images. This is a unique result because single pores were not observed for alamethicin in the lipid monolayer. An example of such individual pores is marked by a red circle in Fig. 2b and Fig. 6 shows a zoomed in image of that pore. In this case, to optimize the hydrophobic–hydrophobic and hydrophilic–hydrophilic interactions the peptide molecules have to orient with their hydrophobic faces towards the lipids and hydrophilic faces towards the center creating a bundle of six peptide molecules that fit into a circle with a radius of 1.5 ± 0.1 nm and forming a central pore with a radius of 0.5±0.05 nm. The inner radius of the hole provides a space for a column of water whose diameter in the trichogin case should be ~0.9 nm. These dimensions are in good agreement with the barrel-stave model of a pore formed by six alpha helical peptides determined by molecular dynamics calculations for bilayers [38]. This study provides direct visual evidence that such aggregation of peptide molecules does take place, indeed. We have used high peptide/lipid ratios to induce the inserted state of the peptide and to have a sufficient number of aggregates to detect their presence in the EC STM image. At this high peptide/lipid ratio we were able to see both large 2D aggregates and single pores. We cannot exclude a possibility, that at the lower peptide/lipid ratios the equilibrium between 2D aggregates and single pores is shifted towards single pore formation.

4. Conclusions

We have described unique EC-STM images of aggregates formed by trichogin OMe incorporated into a phospholipid matrix. The aggregation of trichogin is similar to the previously observed aggregation of alamethicin [26]. Both peptides formed 2D hexagonal nanocrystals. The unit cell of this lattice has a central pore surrounded by six peptide molecules. The two peptides belong to the same class of peptabiotics termed lipopeptaibols known to form transmembrane channels in biological membranes. The EC-STM images shown in this work provide a unique direct visualization of such channels. The similarity in the aggregation of trichogin and alamethicin is a significant result that indicates a similar behavior of the whole class of the lipopeptaibols in phospholipid membranes. Trichogin, however, is shorter than alamethicin. The peptide–peptide interactions are weaker and, consequently, the 2D nanocrystals formed by trichogin are smaller. A particularly interesting consequence is that in the trichogin case single pores formed by a bundle of six TCG molecules were observed in EC-STM images. This result provides the first direct visualization of such a hexameric pore formed by a helical peptide in a phospholipid matrix. The STM data contribute to the ongoing discussion of the nature of the pore formed by TCG molecules in the biological membrane [10,19,21]. They are certainly consistent with the model by Toniolo et al. [10,19] assuming that two antiparallel head-to-head oriented peptides form the channel, as illustrated by Figure 6 in ref [10]. Since our measurements are performed on a monolayer we cannot comment on the effect of thinning of the bilayer proposed by Bobone et al. [21]. However, we are now planning to perform AFM imaging of a bilayer and since membrane thinning in that case must be very pronounced we should be able to see this phenomenon.

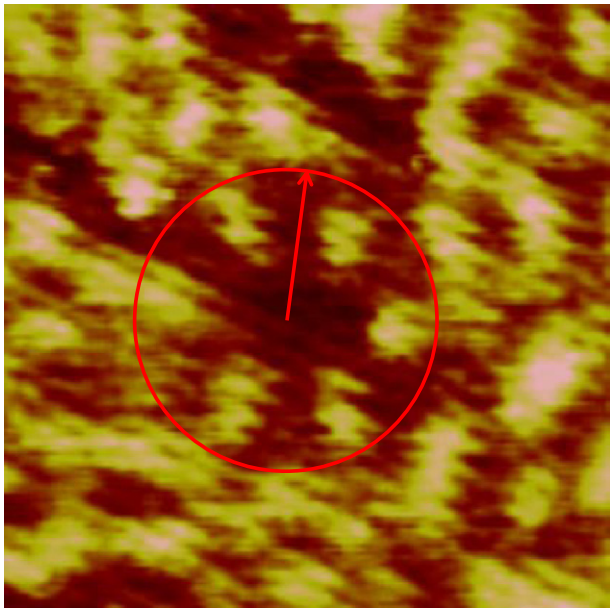

Fig. 6. A 6 × 6 nm^2 molecular resolution EC-STM image of a single pore formed by a bundle of six TCG molecules in the mixed 1:9 TCG:DMPC monolayer in 0.1 M NaF electrolyte recorded at 200 mV vs Ag/AgCl, 350 pA tunneling current, 400 mV bias voltage, and 21 °C temperature.

Acknowledgement

We thank Dr. P. Pieta and Dr. D. Soldatov for helpful discussions, Dr. M. Crisma for crystallographic data of the trichogin and Dr. R.A. Merrill for the help with plotting electrostatic surface potential surfaces of TCG molecule. M.S. and J.L. thank the NSERC (grant number 400523) Discovery Grant for financial support. We express gratitude to anonymous referee of this paper for his suggestions on how to optimize molecular interactions in the model presented in Fig. 5c.

References

[1] K. Brown, R. Hancock, Cationic host defense (antimicrobial) peptides, Curr. Opin. Immunol. 18 (2006) 24–30.
[2] R.E. Hancock, Cationic peptides: effectors in innate immunity and novel antimicrobials, Lancet Infect. Dis. 1 (2001) 156–164.
[3] V. Teixeira, M.J. Feio, M. Bastos, Role of lipids in the interaction of antimicrobial peptides with membranes, Prog. Lipid Res. 51 (2012) 149–177.
[4] G. Bocchinfuso, A. Palleschi, B. Orioni, G. Grande, F. Formaggio, C. Toniolo, Y. Park, K. Hahm, L. Stella, Different mechanisms of action of antimicrobial peptides: insights from fluorescence spectroscopy experiments and molecular dynamics simulations, J. Pept. Sci. 15 (2009) 550–558.
[5] Y. Shai, Mode of action of membrane active antimicrobial peptides, Biopolymers 66 (2002) 236–248.
[6] C. Toniolo, M. Crisma, F. Formaggio, C. Peggion, V. Monaco, C. Goulard, S. Rebuffat, B. Bodo, Effect of N-alpha-acyl chain length on the membrane-modifying properties of synthetic analogs of the lipopeptaibol trichogin GA IV, J. Am. Chem. Soc. 118 (1996) 4952–4958.
[7] C. Auvinguette, S. Rebuffat, Y. Prigent, B. Bodo, Trichogin-A-Iv, an 11-residue lipopeptaibol from trichoderma-longibrachiatum, J. Am. Chem. Soc. 114 (1992) 2170–2174.
[8] M. Crisma, V. Monaco, F. Formaggio, C. Toniolo, C. George, J. Flippen-Anderson, Crystallographic structure of a helical lipopeptaibol antibiotic analogue, Lett. Pept. Sci. 4 (1997) 213–218.
[9] V. Monaco, F. Formaggio, M. Crisma, C. Toniolo, P. Hanson, G. Millhauser, C. George, J. Deschamps, J. Flippen-Anderson, Determining the occurrence of a 3(10)-helix and an alpha-helix in two different segments of a lipopeptaibol antibiotic using TOAC, a nitroxide spin-labeled C-alpha-tetrasubstituted alpha-amino acid, Bioorg. Med. Chem. 7 (1999) 119–131.
[10] C. Toniolo, C. Peggion, M. Crisma, F. Formaggio, X. Shui, D. Eggleston, Structure determination of racemic trichogin-A-Iv using centrosymmetric crystals, Nat. Struct. Biol. 1 (1994) 908–914.
[11] C. Peggion, F. Formaggio, M. Crisma, R. Epand, R. Epand, C. Toniolo, Trichogin: a paradigm for lipopeptaibols, J. Pept. Sci. 9 (2003) 679–689.
[12] C. Toniolo, M. Crisma, F. Formaggio, C. Peggion, R. Epand, R. Epand, Lipopeptaibols, a novel family of membrane active, antimicrobial peptides, Cell. Mol. Life Sci. 58 (2001) 1179–1188.

[13] M. De Zotti, B. Biondi, Y. Park, K. Hahm, M. Crisma, C. Toniolo, F. Formaggio, Antimicrobial lipopeptaibol trichogin GA IV: role of the three Aib residues on conformation and bioactivity, Amino Acids 43 (2012) 1761–1777.
[14] M. De Zotti, B. Biondi, F. Formaggio, C. Toniolo, L. Stella, Y. Park, K. Hahm, Trichogin GA IV: an antibacterial and protease-resistant peptide, J. Pept. Sci. 15 (2009) 615–619.
[15] A. Milov, D. Erilov, E. Salnikov, Y. Tsvetkov, F. Formaggio, C. Toniolo, J. Raap, Structure and spatial distribution of the spin-labelled lipopeptide trichogin GA IV in a phospholipid membrane studied by pulsed electron-electron double resonance (PELDOR), Phys. Chem. Chem. Phys. 7 (2005) 1794–1799.
[16] E.S. Salnikov, D.A. Erilov, A.D. Milov, Y.D. Tsvetkov, C. Peggion, F. Formaggio, C. Toniolo, J. Raap, S.A. Dzuba, Location and aggregation of the spin-labeled peptide trichogin GA IV in a phospholipid membrane as revealed by pulsed EPR, Biophys. J. 91 (2006) 1532–1540.
[17] R. Epand, R. Epand, V. Monaco, S. Stoia, F. Formaggio, M. Crisma, C. Toniolo, The antimicrobial peptide trichogin and its interaction with phospholipid membranes, Eur. J. Biochem. 266 (1999) 1021–1028.
[18] C. Mazzuca, L. Stella, M. Venanzi, F. Formaggio, C. Toniolo, B. Pispisa, Mechanism of membrane activity of the antibiotic trichogin GA IV: a two-state transition controlled by peptide concentration, Biophys. J. 88 (2005) 3411–3421.
[19] V.N. Syryamina, N.P. Isaev, C. Peggion, F. Formaggio, C. Toniolo, J. Raap, S.A. Dzuba, Small-amplitude backbone motions of the spin-labeled lipopeptide trichogin GA IV in a lipid membrane as revealed by electron spin echo, J. Phys. Chem. B 114 (2010) 12277–12283.
[20] C. Heuber, F. Formaggio, C. Baldini, C. Toniolo, K. Mueller, Multinuclear solid-state-NMR and FT-IR-absorption investigations on lipid/trichogin bilayers, Chem. Biodivers. 4 (2007) 1200–1218.
[21] S. Bobone, Y. Gerelli, M. De Zotti, G. Bocchinfuso, A. Farrotti, B. Orioni, F. Sebastiani, E. Latter, J. Penfold, R. Senesi, F. Formaggio, A. Palleschi, C. Toniolo, G. Fragneto, L. Stella, Membrane thickness and the mechanism of action of the short peptaibol trichogin GA IV, Biochim. Biophys. Acta Biomembr. 1828 (2013) 1013–1024.
[22] L. Stella, C. Mazzuca, M. Venanzi, A. Palleschi, M. Didone, F. Formaggio, C. Toniolo, B. Pispisa, Aggregation and water–membrane partition as major determinants of the activity of the antibiotic peptide trichogin GA IV, Biophys. J. 86 (2004) 936–945.
[23] T. Kropacheva, T. Raap, Ion transport across a phospholipid membrane mediated by the peptide trichogin GA IV, Biochim. Biophys. Acta Biomembr. 1567 (2002) 193–203.
[24] L. Becucci, F. Maran, R. Guidelli, Probing membrane permeabilization by the antibiotic lipopeptaibol trichogin GA IV in a tethered bilayer lipid membrane, Biochim. Biophys. Acta (BBA) - Biomembr. 1818 (2012) 1656–1662.
[25] S. Sek, T. Laredo, J.R. Dutcher, J. Lipkowski, Molecular resolution imaging of an antibiotic peptide in a lipid matrix, J. Am. Chem. Soc. 131 (2009) 6439–6444.
[26] P. Pieta, J. Mirza, J. Lipkowski, Direct visualization of the alamethicin pore formed in a planar phospholipid matrix, Proc. Natl. Acad. Sci. U. S. A. 109 (2012) 21223–21227.
[27] M.D. Zotti, B. Biondi, C. Peggion, F. Formaggio, Y. Park, K. Hahm, C. Toniolo, Trichogin GA IV: a versatile template for the synthesis of novel peptaibiotics, Org. Biomol. Chem. 10 (2012) 1285–1299.
[28] R. Volinsky, S. Kolusheva, A. Berman, R. Jelinek, Investigations of antimicrobial peptides in planar film systems, Biochim. Biophys. Acta Biomembr. 1758 (2006) 1393–1407.
[29] B. Gregory, R. Dluhy, L. Bottomley, Structural characterization and nanometer-scale domain formation in a model phospholipid-bilayer as determined by infrared-spectroscopy and scanning-tunneling-microscopy, J. Phys. Chem. 98 (1994) 1010–1021.
[30] M. Li, U. Retter, J. Lipkowski, Kinetic studies of spreading DMPC vesicles at the air–solution interface using film pressure measurements, Langmuir 21 (2005) 4356–4361.
[31] A.H. Kycia, J. Wang, A.R. Merrill, J. Lipkowski, Atomic force microscopy studies of a floating-bilayer lipid membrane on a Au(111) surface modified with a hydrophilic monolayer, Langmuir 27 (2011) 10867–10877.
[32] L. Giancarlo, G. Flynn, Scanning tunneling and atomic force microscopy probes of self-assembled, physisorbed monolayers: peeking at the peaks, Annu. Rev. Phys. Chem. 49 (1998) 297–336.
[33] Y. He, T. Ye, E. Borguet, The role of hydrophobic chains in self-assembly at electrified interfaces: observation of potential-induced transformations of two-dimensional crystals of hexadecane by in-situ scanning tunneling microscopy, J. Phys. Chem. B 106 (2002) 11264–11271.
[34] A.F. Raigoza, J.W. Dugger, L.J. Webb, Review: recent advances and current challenges in scanning probe microscopy of biomolecular surfaces and interfaces, ACS Appl. Mater. Interfaces 5 (2013) 9249–9261.
[35] K. Brogden, Antimicrobial peptides: pore formers or metabolic inhibitors in bacteria? Nat. Rev. Microbiol. 3 (2005) 238–250.
[36] H. Hauser, I. Pascher, R. Pearson, S. Sundell, Preferred conformation and molecular packing of phosphatidylethanolamine and phosphatidylcholine, Biochim. Biophys. Acta 650 (1981) 21–51.
[37] N. Garcia-Araez, C.L. Brosseau, P. Rodriguez, J. Lipkowski, Layer-by-layer PMIRRAS characterization of DMPC bilayers deposited on a Au(111) electrode surface, Langmuir 22 (2006) 10365–10371.
[38] I. Kerr, R. Sankararamakrishnan, O. Smart, M. Sansom, Parallel helix bundles and ion channels — molecular modeling via simulated annealing and restrained molecular-dynamics, Biophys. J. 67 (1994) 1501–1515.
[39] W.L. DeLano, The PyMOL Molecular Graphics System, Version 1.5.0.4 Schrödinger, LLC, 2002. www.pymol.org.
[40] S. Iftemi, M. De Zotti, F. Formaggio, C. Toniolo, L. Stella, T. Luchian, Electrophysiology investigation of trichogin GA IV activity in planar lipid membranes reveals ion channels of well-defined size, Chem. Biodivers. 11 (2014) 1069–1077.